PHYSICAL REVIEW B VOLUME 58, NUMBER 18 1 NOVEMBER 1998-II

Ab initio molecular dynamics of expanded liquid sodium

S. R. Bickham
Theoretical Division, Los Alamos National Laboratory, Los Alamos, New Mexico 87545

O. Pfaffenzeller
Institut für Festkörperforshung Forschungszentrum Jülich, D-52425 Jülich, Germany

L. A. Collins and J. D. Kress
Theoretical Division, Los Alamos National Laboratory, Los Alamos, New Mexico 87545

D. Hohl*
Institut für Festkörperforshung Forschungszentrum Jülich, D-52425 Jülich, Germany

(Received 7 April 1998)

The properties of liquid sodium have been studied using *ab initio* molecular dynamics over a wide range of temperatures and pressures. When expanded along the liquid-vapor coexistence curve, the dc conductivity and average number of nearest neighbors decrease, as has been observed for other alkali metals. There is a sharp drop in the dc conductivity when the density decreases from 0.31 to 0.16 g/cm^3. For densities at or below the latter value, the sodium vapor was observed to partially condense into a small fraction of the supercell simulation volume. This condensation was accompanied by aggregation of sodium atoms, but the lifetimes of these clusters are less than the vibrational period of the sodium dimer, indicating that they are short-lived transient associates, not molecular clusters in the traditional sense. [S0163-1829(98)50242-1]

The properties of liquid alkali metals along the liquid-vapor coexistence curve have received considerable attention in recent years. At high densities, near the triple point, these materials may be regarded as monatomic conducting fluids with each atom contributing one electron to a conduction band.[1] As the alkali is expanded along the coexistence curve, the dc conductivity and average number of nearest neighbors both decrease, while the average nearest neighbor separation remains relatively constant.[2] Near the critical point, there is a sharp drop in the dc conductivity as the fluid undergoes a metal-non-metal (MNM) transition.[3] The critical point may also be approached from below by condensing the vapor. In this case a transition from a nonconducting mixture of atoms and molecules to a conducting atomic liquid should occur.

Most of the experimental and theoretical studies of expanded alkali metals have been restricted to rubidium and cesium due to the accessibility of the critical conditions, $T_c = 1924$ K and $P_c = 9.25$ MPa for Cs and $T_c = 2017$ K and $P_c = 12.45$ MPa for Rb.[3] These have generally concluded that the origin of the MNM transition is correlated with the formation of molecular clusters. For example, an examination of equation-of-state data of cesium near the critical point concluded that there is a substantial number of dimers and tetramers,[4] while another calculation suggests that the stable structure resulting from the expansion of a bcc cesium lattice is a simple cubic lattice of cesium dimers.[5] The appearance of low frequency harmonic oscillations in the structure factor of expanded cesium[6] and rubidium[7] also gives evidence for an atomic to molecular transition in the fluid. The properties of liquid sodium in this region are not as well documented due to the difficulty in reaching the critical point, $T_c = 2485$ K and $P_c = 24.8$ MPa.[3]

There have been several studies of these systems using classical molecular dynamics (MD) simulations, but these are of little use in predicting properties near the critical point since the variations in the electronic and ionic degrees of freedom cannot be accurately modeled with an empirical potential. For this reason, an increasing number of first principles, *ab initio* or quantum MD simulations have been used to investigate the properties of liquid alkali metals. Many of these are still restricted to temperatures and densities well below the critical point.[8–12] Among the more general studies are calculations of the radial distribution and optical conductivity in expanded rubidium at 350 and 1400 K using the local density approximation (LDA) in combination with a MD simulation.[13,14] A similar technique was used by Silvestrelli, Alavi, and Parrinello to calculate the pair correlation and optical conductivity in liquid sodium at temperatures up to 1000 K.[15] Self-diffusion constants in liquid sodium at temperatures ranging from 400 to 1400 K were also calculated in *ab initio* simulations based on the Car-Parrinello formalism.[16] Simulations based on first principles have also been used to calculate the radial distribution function, diffusivity and other properties of cesium and rubidium, but the lowest densities in this study were approximately four times the critical values.[17]

In this Rapid Communication, we present the results of *ab initio* MD simulations of liquid sodium at fixed densities of 0.08, 0.16, 0.31, 0.47, 0.74, and 1.28 g/cm^3 and temperatures ranging from 800 to 3000 K. Our simulations cover a much wider range of densities and temperatures than has previously been explored either experimentally or theoretically. We use MD to generate ionic trajectories and compute the forces acting on the classical ions

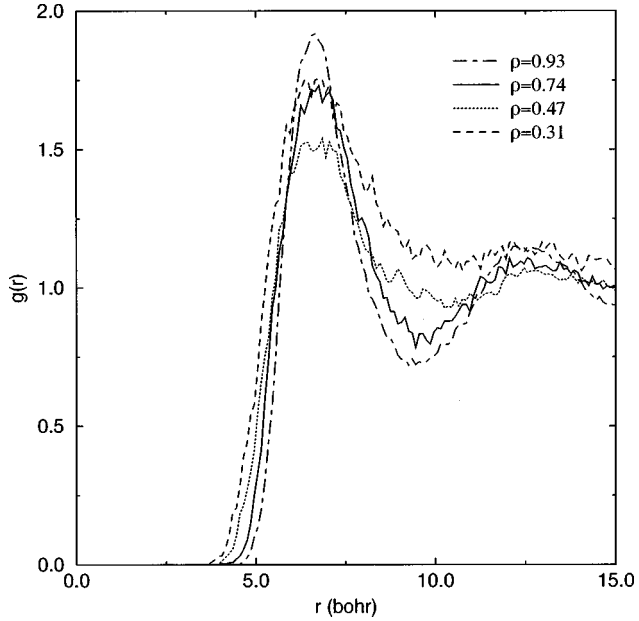

FIG. 1. Radial distribution function for four points near the liquid-vapor coexistence curve. The temperatures, peak positions, and number of nearest neighbors for each density are given in Table I.

$$M_I \ddot{\vec{R}}_I = -\nabla_{\vec{R}_I} E_{\mathrm{DFT}} \tag{1}$$

from first principles using Hohenberg-Kohn-Sham density functional theory[18] (DFT) in the local density approximation (LDA). Note that 1.28 g/cm^3 is the LDA equilibrium density, while 0.93 g/cm^3 is the experimentally observed equilibrium density. The LDA has a well-known tendency to overbind weakly interacting atoms.

To compute the *ab initio* trajectories we use the Car-Parrinello method, for which numerous reviews are available.[19] The fictitious masses μ_i for the electronic wave functions, ψ_i, were $\mu = 300$ a.u. and the time step sizes were $\Delta t = 7$ a.u.. We use a simple cubic unit cell with periodic boundary conditions containing 64 ($\rho = 0.08$ g/cm^3) and 128 atoms (all other densities). The plane wave cut-off energy in the expansion of the ψ_i was 6 Ry at the Gamma point ($k = 0$) in the Brillouin zone of the supercell. The electron-ion interaction is represented by a Martins-Troullier type local pseudopotential.[20] The MD trajectories comprise 750–5000 (microcanonical) time steps after careful equilibration.

We have performed many careful checks on the quality of the interaction and simulations. For the heavily-studied region around melt ($\rho \sim 0.93$ g/cm^3; $T = 500$–1000 K), our pair-correlation functions, diffusion coefficients, and electrical conductivities compared very well with experimental values[21] and other *ab initio* MD simulations.[15,16] In addition, analysis of the post-equilibration trajectories indicates that quantities such as the autocorrelation functions, for example, have reached stable forms yielding statistically meaningful properties.

The radial distribution function, $g(r)$, was calculated by averaging over the atomic positions during each trajectory. It is plotted in Fig. 1 for four points near the liquid-vapor coexistence curve, as mapped out in Ref. 21. Note that these densities are above the critical value of 0.30 g/cm^3. The temperature dependence of $g(r)$ is similar to that found for other liquid alkali metals in experiments[2] and density functional MD simulations.[17] At low temperatures, there is a strong primary peak that becomes broader and less intense with increasing temperature. The position of this peak, R_1, remains nearly constant. However, the average number of nearest neighbors, defined by $N_1 = 2\rho \int_0^{R_1} g(r) 4\pi r^2 dr$, where ρ is the density, decreases with decreasing density, as shown in Table I. The usual interpretation of this behavior is that the density decreases by reducing the average number of neighbors, not by increasing the average interatomic separation.[2] A second peak is also evident at higher densities, but this gradually becomes washed out due to a reduction in the average number of second nearest neighbors in the atomic fluid.

TABLE I. Liquid sodium properties near the coexistence curve. See text for definitions of R_1 and N_1.

ρ (g/cm^3)	T (K)	R_1 (bohr)	N_1	σ_0 (10^3 Ω^{-1} cm^{-1})
0.93	800	6.64	6.4	38
0.74	1200	6.69	5.4	8.3
0.47	2100	6.62	3.3	2.7
0.31	2500	6.65	2.7	1.4

The dc conductivity was also calculated for selected trajectories using Γ point sampling in the Kubo-Greenwood formulation,[22,23] with the usual delta function resolved by averaging over a finite frequency interval, $\Delta\omega$, giving[24,25]

$$\sigma(\omega) = \frac{2\pi}{\Omega \Delta\omega} \sum_{ij} \frac{F[\epsilon_i, \epsilon_j] |D_{ij}|^2}{\epsilon_j - \epsilon_i} \tag{2}$$

where Ω is the atomic volume. $F[\epsilon_i, \epsilon_j] = [f_0(\epsilon_i) - f_0(\epsilon_j)]/\omega$, which is the difference between the Fermi-Dirac distributions f_0 at temperature T and frequency ω. $|D_{ij}|^2 = \frac{1}{3}\Sigma_\alpha |\langle \psi_i | \nabla_\alpha | \psi_j \rangle|^2$, which represents the velocity dipole matrix element. The quantities ϵ_i and ψ_i are the energy and wave functions for the ith orbital found from the diagonalization of the Kohn-Sham equations. The summation in i runs over all occupied states while that in j covers only unoccupied states. The dc conductivity is then obtained by averaging $\sigma(\omega)$ over several time steps and using a polynomial fit to extrapolate to zero frequency. We note that Silvastrelli, Alavi, and Parrinello calculated the electrical conductivity of liquid sodium for temperatures up to 1000 K using both Γ point and 8-k vector sampling.[15] There was good agreement between the two sampling methods at temperatures above 850 K, so the Γ-point sampling in our calculations should yield sufficient accuracy.

Table I gives the value of the dc conductivity for four points on the coexistence curve, indicating that it decreases monotonically with decreasing density. A similar analysis is more difficult at lower densities due to the large supercell size and concomitant computational effort; however a calculation at 0.16 g/cm^3 yields a dc conductivity on the order of 100 Ω^{-1} cm^{-1}, which is approximately the size of the error bars in the extrapolation of $\sigma(\omega)$. This value is an order of magnitude smaller than the calculated dc conductivity at a density of 0.31 g/cm^3 and a temperature of 2500 K, which

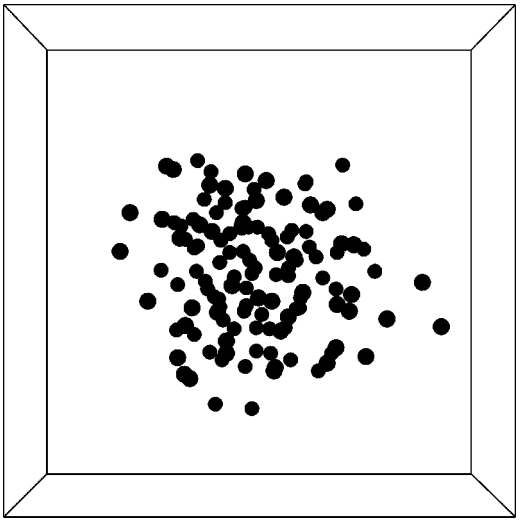

FIG. 2. A snapshot of atomic positions at 1000 K and a density of 0.16 g/cm^3. The supercell size is defined by the box.

indicates that the critical point in our simulations is below 0.31 g/cm^3 and is consistent with the critical density of 0.30 g/cm^3 reported for sodium.[3]

The temperature and density dependence of $g(r)$ and the average number of nearest neighbors provide a rather coarse-grained description of the physical characteristics of the system. To determine how the atoms interact, it is more instructive to examine movies of the simulations. Snapshots taken from such a movie are shown in Figs. 2 and 3 for a density of 0.16 g/cm^3 (128 atoms) and temperatures of 1000 and 2500 K, respectively. The atomic positions are plotted with solid circles, while the box represents the size of the periodic supercell. At the higher temperature, the atoms are fairly well distributed in the simulation volume, although there are some sizable regions with a lower instantaneous density. This feature is more pronounced in the snapshot at 1000 K, with all of the atoms occupying a volume that is approximately 25% of the supercell size. This corresponds to a density of approximately 0.64 g/cm^3, which is very close to the density of the liquid at this temperature.[21]

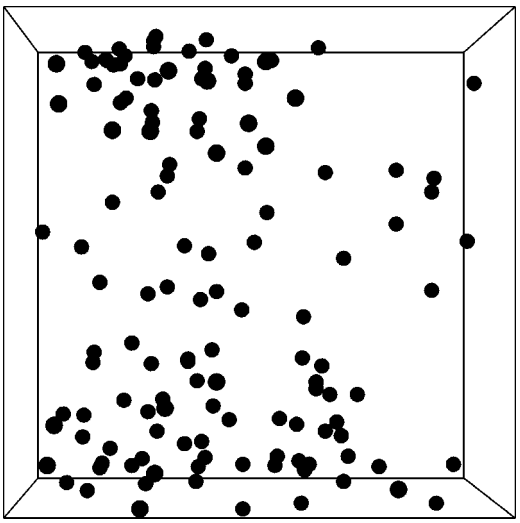

FIG. 3. A snapshot of atomic positions at 2500 K and a density of 0.16 g/cm^3. The supercell size is defined by the box.

This striking condensation was also observed at the lowest density studied, 0.08 g/cm^3 (64 atoms) at a temperature of 2100 K, but not at 2300 K. These values bracket the experimental equation-of-state curve for sodium vapor. There appears to be a tendency for the system to liquefy at densities below the critical density, but inside the coexistence curve. No condensation occurred in the trajectories at densities greater than 0.30 g/cm^3 at any temperature. The movies show that the atoms are, on the average, uniformly distributed throughout the supercell for the duration of the simulation. The phase separation behavior that we observe in our fixed-volume simulations is expected for the two-component region (vapor/liquid) and reasonable. However, we cannot expect the simulated phase separation to occur on the coexistence line. Surface effects in such small droplets will be unrealistically large, and the finite duration of the simulations will prevent the thermodynamically most stable phases to be reached. What we instead see is very likely a *kinetic* instability. More simulations with larger samples and longer trajectories need to be performed at the lower densities to understand the conditions that lead to condensation of the atomic vapor.

We note that a visual analysis of the simulation is not required to detect the onset of condensation. In a cubic supercell, evaluation of the radial distribution function is limited to a sphere with a radius equal to half of the supercell diameter. Therefore, only a fraction, $4\pi(L/2)^3/3L^3=0.52$, of the atoms are included in the averaging for a uniform spatial distribution. The integrated $g(r)$, $I=(1/V)\int_0^{R_2} g(r)4\pi r^2 dr$, should then be equal to 0.52, where V is the volume ($=L^3$), and $R_2=L/2$. In the simulations reported here, $I\leqslant 0.58$ for all cases except those at densities below the critical density, but inside the coexistence curve, as noted above. In the trajectories corresponding to Figs. 2 and 3, $I=0.84$ and 0.63, respectively, while $I=0.73$ for the 0.08 g/cm^3, $T=2100$ K simulation mentioned above. Therefore, an integrated $g(r)$ significantly larger than the value for a uniform distribution of atoms can indicate the degree of condensation.

An important physical change that has been observed in liquid alkali metals near the critical point is the formation of diatomic molecules.[6,7] The formation of these dimers and more complex molecules is analyzed in our simulations by identifying the atoms within a distance, r_c, of each atom and monitoring the evolution of each cluster. We found that the most physical results are obtained by setting $r_c=R_1$, the center of the first peak in $g(r)$. Although this may seem a little conservative, larger radii generally produce a flat distribution of cluster sizes and a significant number of clusters of size $N/4$ or larger. Smaller radii result in a very high percentage of single atoms.

The lifetimes of these clusters are calculated by comparing the clusters in successive time steps to determine how long they remain intact. For each trajectory, the dimer is found to have the longest average lifetime, ranging from 0.94 τ_{Na} at 0.08 g/cm^3 and 2300 K to 0.37 τ_{Na} at 1.28 g/cm^3 and 800 K, where $\tau_{\mathrm{Na}}=210$ fs is the vibrational period of the diatomic sodium molecule. The trimer lifetimes are reduced by approximately 30% from these values, and the lifetime decreases rapidly with further increases in the cluster size. The fact that these lifetimes are less than the vibrational pe-

riod of a Na_2 molecule indicates that although a significant number of atoms are close enough to strongly interact at a given time, these clusters do not retain their identities long enough to be considered molecules.

Similar transient aggregation was observed in liquid high-density hydrogen.[24–26] Such behavior is in contrast to a study of expanded cesium in which the structure factor was modeled using reverse Monte Carlo techniques.[27] This method produces a snapshot of the average atomic configuration, but the dynamical properties need to be taken into account to ensure that the lifetimes are significant with respect to the molecular vibrations.

In conclusion, we have used Car-Parrinello simulations to study the properties of expanded liquid sodium for a wide range of densities and temperatures. The decrease in the dc conductivity and number of nearest neighbors with decreasing density along the liquid-vapor coexistence curve is in good agreement with the experimental results found for other liquid alkali metals.[2] A cluster analysis shows that a significant number of dimers and other molecules exist at a given time step, but the lifetimes are much less than the vibrational period of Na_2. An interesting condensation was observed in several simulations at densities below the critical value, but inside the coexistence curve. To the best of our knowledge, this behavior has not been found in other simulations of expanded alkali metals.

This work was performed under the auspices of the U.S. Department of Energy through the Theoretical Division of the Los Alamos National Laboratory. We acknowledge valuable discussions with Dr. L. Pratt of Los Alamos.

*Permanent address: Shell E&P Technology Co., Houston, TX 77001-0481.

[1] N. W. Ashcroft, Nuovo Cimento D **12**, 597 (1990).

[2] R. Winter, F. Hensel, T. Bodensteiner, and W. Gläser, Ber. Bunsenges. Phys. Chem. **91**, 1327 (1987).

[3] F. Hensel, J. Phys.: Condens. Matter **2**, SA33 (1990).

[4] C. T. Ewing, J. P. Stone, J. R. Spann, and R. R. Miller, J. Phys. Chem. **71**, 473 (1967).

[5] M. Ross, L. Yang, B. Dahling, and N. Winter, Z. Phys. Chem. (Munich) **184**, 65 (1994).

[6] W.-C. Pilgrim, R. Winter, and F. Hensel, J. Phys.: Condens. Matter **5**, B183 (1993).

[7] W.-C. Pilgrim, M. Ross, L. H. Yang, and F. Hensel, Phys. Rev. Lett. **78**, 3685 (1997).

[8] J. Theilhaber, Phys. Rev. B **46**, 12 990 (1992).

[9] F. Shimojo, K. Hoshino, and M. Watabe, J. Phys. Soc. Jpn. **63**, 141 (1994).

[10] M. Foley, E. Smargiassi, and P. A. Madden, J. Phys.: Condens. Matter **6**, 5231 (1994).

[11] D. L. Lynch, N. Troullier, J. D. Kress, and L. A. Collins, J. Chem. Phys. **101**, 7048 (1994).

[12] F. Shimojo, Y. Zempo, K. Hoshino, and M. Watabe, Phys. Rev. B **55**, 5708 (1997).

[13] K. Hoshino and F. Shimojo, J. Phys.: Condens. Matter **8**, 9315 (1996).

[14] F. Shimojo, Y. Zempo, K. Hoshino, and M. Watabe, Phys. Rev. B **52**, 9320 (1995).

[15] P. L. Silvestrelli, A. Alavi, and M. Parrinello, Phys. Rev. B **55**, 15 515 (1997).

[16] G. X. Qian, M. Weinert, G. W. Fernando, and J. W. Davenport, Phys. Rev. Lett. **64**, 1146 (1990).

[17] B. J. C. Cabral and J. L. Martins, Phys. Rev. B **51**, 872 (1995).

[18] For a review, see R. O. Jones and O. Gunnarsson, Rev. Mod. Phys. **61**, 689 (1989).

[19] For reviews, see D. K. Remler and P. A. Madden, Mol. Phys. **70**, 921 (1990); G. Pastore, E. Smargiassi, and F. Buda, Phys. Rev. A **44**, 6334 (1991); T. Oguchi and T. Sasaki, Prog. Theor. Phys. Suppl. **103**, 93 (1991); M. C. Payne, M. P. Teter, D. C. Allan, T. A. Arias, and J. D. Joannopoulos, Rev. Mod. Phys. **64**, 1045 (1992); G. Galli and M. Parrinello, in *Computer Simulation in Materials Science*, edited by M. Meyer and V. Pontikis (Plenum, New York, 1991), p. 283; D. Hohl, Theor. Chim. Acta **91**, 237 (1995).

[20] N. Troullier and J. L. Martins, Phys. Rev. B **43**, 1993 (1991).

[21] V. A. Alekseev and T. Iakubov, *Handbook of Thermodynamic and Transport Properties of Alkali Metals*, edited by R. W. Ohse (Blackwell Scientific, Oxford, 1985), Chap. 7.1.

[22] W. A. Harrison, *Solid State Theory* (McGraw-Hill, New York, 1970).

[23] N. W. Ashcroft and N. D. Mermin, *Solid State Physics* (Saunders, Philadelphia, 1976).

[24] I. Kwon, L. Collins, J. Kress, and N. Troullier, Phys. Rev. E **54**, 2844 (1996).

[25] O. Pfaffenzeller and D. Hohl, J. Phys.: Condens. Matter **9**, 11 023 (1997).

[26] O. Pfaffenzeller, thesis IFFF, Jülich, 1996.

[27] V. M. Nield, M. A. Howe, and R. L. McGreevy, J. Phys.: Condens. Matter **3**, 7519 (1991).